# Radical-Pair Dynamics in the Photoreduction of Anthraquinone in Sodium Dodecyl Sulfate Micellar Solution Detected by Pulse-Mode Product-Yield-Detected Electron Spin Resonance: Temperature and Salt Dependence†

**Nicolai E. Polyakov,‡ Masaharu Okazaki,* Yoshinari Konishi, and Kazumi Toriyama**

*National Industrial Research Institute of Nagoya, Hirate, Kita-ku, Nagoya 462, Japan*

*Received: May 24, 1995; In Final Form: July 24, 1995*®

The dynamical behavior of the radical pair (RP) produced in the photoreduction of anthraquinone in sodium dodecyl sulfate (SDS) micellar solutions has been observed at various temperatures and salt concentrations by using the pulse-mode product-yield-detected ESR (PYESR) technique. Through the numerical calculation of the time-domain PYESR response by the Runge−Kutta method applied to a reaction scheme, dynamical parameters such as the escape rate of the RP ($k_{ESC}$) and the rate of spin trapping directly from the RP ($k_{ST}$) have been obtained. Since these kinetic parameters are very informative for elucidating the micelle dynamics, we may call this method the "spin-pair-probe" technique.

## 1. Introduction

A large number of papers have been published on the magnetic field effect (MFE) in various kinds of chemical reactions,[1−4] which were detected mainly by the transient absorption method[5,6] and product analysis.[7,8] The radical pair model of CIDNP[9,10] has been proposed for the mechanism of this magnetic field dependence and was confirmed by several techniques. For the photoreduction of quinones in sodium dodecyl sulfate (SDS) micellar solutions, we found that the ESR transitions of both the SDS radical and the semiquinone radical affect the yield of a product that is produced only from the SDS radical (i.e. spin adduct).[11] This is direct evidence of the RP model for this kind of magnetic field dependence. As another evidence of the RP model, Closs et al.[12] and McLauchlan et al.[13] have explained a new-type of CIDEP found by Sakaguchi et al.[14] for a similar system with the interaction in the RP. Because with our method the ESR spectrum of the RP is traced by the change of the final-product yield, we call this method product-yield-detected ESR,[15,16] or PYESR in short. Since these spin-dependent phenomena are deeply concerned with the relation between the chemical bond and the spin correlation of the two unpaired electrons from which a new bond is created,[17] these are undoubtedly an important theme of the basic chemistry.

In the PYESR technique, we usually use the spin trapping method[18,19] to separate the escape product as a spin adduct from the cage product, and also to determine the yield by ESR with which in-situ observation is easy. Since PYESR is also possible by using the HPLC method,[20] other techniques such as NMR should be potentially applicable. As a similar technique to detect the ESR of a spin pair,[21] the optically-detected ESR technique has been well-known in solid-state physics[22−24] and subsequently applied to solution chemistry.[25−29] These studies have been successful in elucidating the structure of ionic species in the irradiated systems,[25,26,29] the reaction mechanism of the photosynthetic system,[27] and the dynamics of an ion pair in a photolytically ionized system.[28] The main difference with our method is that we observe the yield of a final product and the vertical axis of PYESR represents the yield, thus sometimes measured in M/L, whereas the optical detection technique monitors photons of less than $10^6$, emitted upon recombination of the pair of ions to return to the neutral states (i.e., atoms or molecules). As another technique which is similar to our method, CIDNP-detected ESR[30] was successful in discussing the process of photochemical reactions which have RPs as the intermediates. Recently, we have presented a new pulse-mode version of the PYESR technique[16,31−33] to obtain the kinetic parameters of the RP produced in the photolysis of carbonyl compounds in micellar solutions. The Runge−Kutta method is employed to simulate the "pulse-PYESR response" by integrating the differential equations made for the reaction scheme. Through this simulation the rate constants of, e.g., RP formation ($k_H$), escape of the RP ($k_{ESC}$), spin trapping directly from the RP ($k_{ST}$), and cage recombination ($k_P$) can be estimated. We believe that this method plays an important role in the development of "supramolecular spin chemistry"[17] through reliable measurements of the RP lifetime as well as the absolute rate of the escape process from the micelle, which are indispensable as Turro et al. discussed.[17]

In a previous paper,[34] by using the pulse-PYESR technique, we determined $k_{ESC}$ and $k_{ST}$ for the photoreduction of anthraquinone in SDS micellar solution at various concentrations and showed that the two processes contribute to the escape rate of the RP: one is SDS monomer exchange between the micelle and the aqueous bulk phase and the other is a fusion/fission process of the micelles. Contribution of the latter process is small at a low SDS concentration less than 0.1 M, but at a higher concentration it becomes very important. We also showed that the p$K_a$ value of a supramolecular system with a semiquinone of anthraquinone-$\beta$-carboxylic acid and a spherical micelle can be obtained by plotting the escape rate of the RP as a function of pH.[35] These studies gave a new insight into the micelle dynamics by monitoring the spin-pair dynamics, thus we call this method the "spin-pair probe" technique. In the present study, we have applied the pulse-PYESR method to investigate the effect of temperature and salt on the dynamics of the RP produced in the photolysis of anthraquinone (AQ) in SDS micellar solution. It is well-known that a change in the temperature and the addition of an ionic species give profound effects on the micelle character.[36−39] For example, addition of salt changes the shape, the electrostatic character, and the internal viscosity of the micelle. These changes should give

† Abbreviations: RP, radical pair; PYESR, product-yield-detected ESR. MFE, magnetic field effect; CIDEP, chemically induced dynamic electron spin polarization; CIDNP, chemically induced dynamic nuclear polarization; HPLC, high-performance liquid chromatography.

‡ AIST fellow, Oct 1993−Oct 1994. Permanent address: Institute of Chemical Kinetics and Combustion, Novosibirsk 630090, Russia.

® Abstract published in *Advance ACS Abstracts,* September 1, 1995.

0022-3654/95/2099-15108$09.00/0 

**CHART 1**

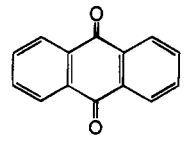

anthraquinone (AQ)

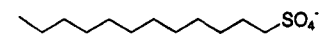

sodium dodecyl sulfate (SDS)

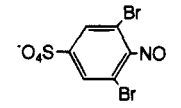

3,5-dibromo-4-nitorosobenzene sulfonate

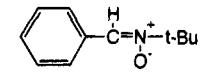

phenyl-t-butyl nitrone (PBN)

effects on the spin-pair dynamics in the micelle. Thus, we would like to show that our technique is very powerful in detecting these effects in the micellar system.

## 2. Experimental Section

Anthraquinone (AQ) purchased from Wako Pure Chemicals (Tokyo) was recrystallized from ethanol. A water-soluble spin trap, sodium 3,5-dibromo-4-nitrosobenzenesulfonate (DBNBS) was synthesized by oxidation of sodium 3,5-dibromosulfanilate obtained from Aldrich Chemical.[40] Sodium dodecyl sulfate (SDS: the purest grade) from Nakarai Chemicals (Kyoto), NaCl of guaranteed grade from Wako Pure Chemicals, and phenyl-*tert*-butylnitrone (PBN) from Aldrich Chemical were used without further purification. AQ was dissolved in 0.1 M SDS/water at 0.06 mM and DBNBS was added to the solution at 1.0 or 3.0 mM just before the experiment. The molecular structures of the above chemicals used in the present study are given as Chart 1. The sample solution was deoxygenated by Ar-gas bubbling for 40 min, supplied to a quartz flat cell set in the ESR cavity with a flow system, and irradiated with a Nd:YAG laser (Spectra-Physics, GCR-150, $\lambda$ = 355 nm, 20 mJ/pulse, 10 Hz) for 30 s. Spin-adduct yield was determined from the amplitude of the ESR spectrum observed with an ESR spectrometer (JEOL, JES-RE1X) 30 s after the laser irradiation. For the time-domain measurement of the microwave effect, a microwave (X-band) was pulsed with a pin switch (HP33142A with a driver HP33190B) and amplified to about 10 W by a TWT amplifier (Keltech Florida, XR 625-20). The laser and the microwave pulses were controlled with a pulse programmer (Iwatsu, SY8220) and a personal computer (NEC, PC9801). Details of the apparatus have been described elsewhere.[16,20]

## 3. Reaction System and the Model

**3.1. Reaction Scheme and the Spin Dependent Phenomena.** The reaction scheme of the present system is as follows:

$$Q + h\nu \rightarrow {}^1Q^* \rightarrow {}^3Q^* \quad (1)$$

$${}^3Q^* + RH \rightarrow {}^3(QH^{\bullet}\ {}^{\bullet}R) \quad (k_H) \quad (2)$$

$${}^3(QH^{\bullet}\ {}^{\bullet}R) \leftrightarrow {}^1(QH^{\bullet}\ {}^{\bullet}R) \quad (k_{ISC}) \quad (3)$$

$${}^1(QH^{\bullet}\ {}^{\bullet}R) \rightarrow \text{cage product} \quad (k_P) \quad (4)$$

$${}^{1,3}(QH^{\bullet}\ {}^{\bullet}R) \rightarrow {}^{\bullet}QH + {}^{\bullet}R \quad (k_{ESC}) \quad (5)$$

$$R^{\bullet} + ST \rightarrow \text{spin adduct} \quad (6)$$

$${}^{1,3}(QH^{\bullet}\ {}^{\bullet}R) + ST \rightarrow \text{spin adduct} \quad (k_{ST}) \quad (7)$$

$$2QH^{\bullet} \rightarrow Q + QH_2 \quad (8)$$

Symbols in the parentheses represent the rate constants of the corresponding processes. The excited triplet state of anthraquinone is produced via the excited singlet state through intersystem crossing (1). It abstracts a hydrogen atom from an SDS molecule to produce a RP in the triplet state, which consists of a semiquinone and an SDS radical (2). One part of the RPs disappears due to cage reactions (4), such as recombination in the original micellar cage after intersystem crossing from $T_0$ to $S$ (3). The other part of the RPs (in $T_{\pm 1}$) decays by diffusion of one of the radicals out of the micelle (escape process (5)). Most of the escaped SDS radicals are converted into spin adducts by the spin trapping reaction (6),[41,42] whose rate is usually rapid enough compared with the competing reactions; thus a constant value of $2.0 \times 10^9$ was employed in the simulation. Direct trapping of the SDS radical from the RP is also possible (7).[32,35] The escaped semiquinone may undergo several reactions, one of which is the disproportionation (8). Although this reaction should be dependent on the magnetic field, it proceeds in a time scale of seconds and does not give an appreciable effect on our observation. It should be mentioned that the spin adduct of the semiquinone radical has not been detected in these systems. This may be due to a low reactivity of the oxygen-centered radical to this spin trap. If other quenching processes exist for the excited triplet quinone in addition to hydrogen abstraction, the rate of appearance of the RP is equal to the decay rate of $^3Q^*$ rather than the hydrogen abstraction rate.

Under the magnetic field three sublevels of the triplet RP are separated energetically by the Zeeman effect, thus intersystem crossing occurs rapidly only between $T_0$ and $S$. Therefore, the RP in one of these two spin states disappears rapidly by the cage reactions. We divide the spin states of a RP into two groups: the $T_0$ and the $S$ levels characterized with a short lifetime and the $T_{+1}$ and the $T_{-1}$ levels with a long lifetime.[43-45] At zero field, however, intersystem crossing occurs efficiently also between $T_{\pm}$ and $S$; thus the RP decays rapidly by the cage reactions regardless of its spin state. Therefore if the initial spin state of the RP is the triplet state, the magnetic field causes a decrease in the yield of cage products and an increase in the yield of spin adducts, which are produced in processes (5)−(7) as the escape product (magnetic-field effect on the spin-adduct yield). Under these circumstances when the ESR transitions are induced between $T_{\pm}$ and $T_0$, intersystem crossing (3) is accelerated, and thus the spin-adduct yield decreases. Therefore, by changing the magnetic field stepwise, the ESR spectrum of the RP can be detected as the changes in the spin-adduct yield (PYESR spectrum).[11,15,32]

**3.2. Pulse-PYESR Experiments.**[16,31,32] Two pulse sequences are shown as insets in Figure 1 with experimental results for the AQ/SDS system at 289 K (circles) and 328 K (squares). In experiment 1 (upper), microwave irradiation starts before the laser pulse and stops $t$ s after the laser pulse. The microwave effect grows with $t$ and finally reaches a plateau value. Two processes mainly contribute to the rate of this growth:[32] one is the formation rate of the RP and the other is the rate of appearance of the population difference between $T_0$ and $T_{\pm}$. The latter rate is also essential, since a population difference is necessary for the ESR transition which modifies the product yield. In experiment 2 (lower), microwave irradiation starts $t$ s after the laser pulse but the irradiation period is kept constant (20 $\mu$s). Since the PYESR response is due to the ESR transitions of the RP, not those of escaped radicals, we observe a decay curve for the PYESR response as a function of $t$. It should be pointed out that cage reactions of the RP whose spin state is originally in the $T_0$ state contribute little to this decay, since

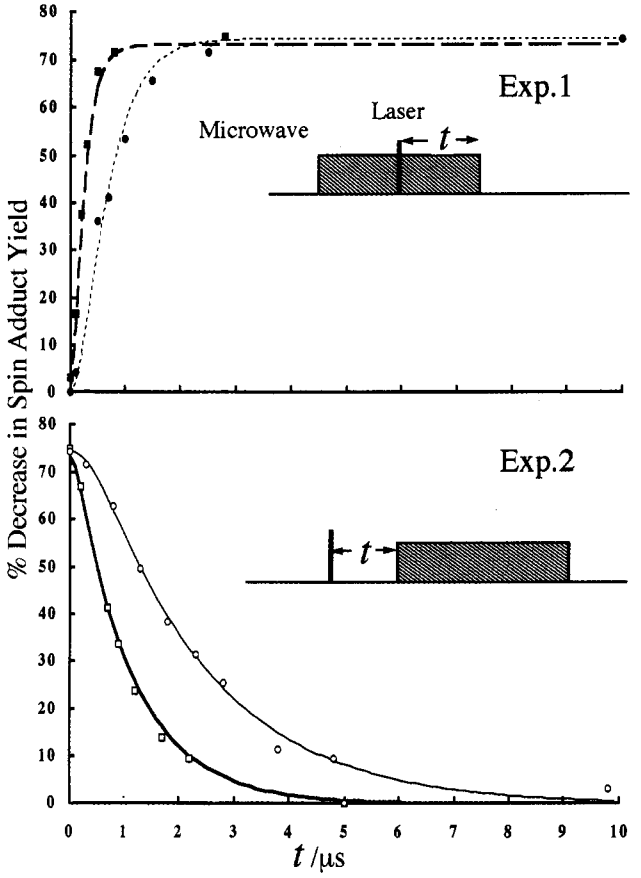


**Figure 1.** Pulse PYESR responses observed for the photoreduction of anthraquinone in a 0.1 M SDS micellar solution with DBNBS added as the spin trap. Two time-domain signals, experiment 1 (upper) and experiment 2 (lower), are obtained with the pulse sequences indicated as the insets. Circles and squares are the experimental results at 289 and 328 K, respectively. Thick and thin lines are the respective simulations with the method described in the text.

the RP in the $T_0$ state usually recombines sooner or later via the $S$ state. The RP in one of the $T_\pm$ states disappears via[16,32,35] (1), a cage reaction after relaxation to either the $T_0$ or the $S$ state, (2) escape of one of the component radicals from the micelle, or (3) spin trapping of the SDS radical which is forming a RP in the micelle. Thus, the rate of "decay" of the microwave effect is approximately the sum of the rates of these three processes, if the "decay process" of experiment 2 proceeds much slower than the "growth" of experiment 1. If the formation rate of the RP, for example, is comparable to or larger than that of the decay process, the former process also contributes to the transient curve of experiment 2. Because one of the components of the RP is an SDS radical which behaves in the same way as an SDS monomer, we can elucidate the micelle dynamics through observing and analyzing the dynamics of the RP.

**3.3. Simulation and Parameters.** Differential equations for the reaction steps (2)−(7) are numerically integrated using the Runge−Kutta method to simulate the pulse-PYESR response. The validity of this classical technique for the simulation of an essentially quantum-mechanical phenomenon has been discussed elsewhere.[32] In this simulation, we have to input three parameters which are not obtained in the present method: electron spin relaxation $k_{RLX}$,[43−45] intersystem crossing $k_{ISC}$, and transition rate due to the microwave effect. All the spin relaxation rates $k_{RLX}$ between the sublevels ($T_0$ and $S$) and ($T_+$ and $T_-$) are postulated to be equal and may be given as follows:[46]

$$k_{RLX} = \gamma^2 \tau_c H_L^2/(1 + \omega^2 \tau_c^2) \qquad (9)$$

where $\gamma$ represents the gyromagnetic ratio of the electron spin, $H_L$ and $\tau_c$ are the fluctuating field and its correlation time, and $B_0$ is the external magnetic field (thus $\omega = \gamma B_0$). Since several contributors are considered for $H_L$, an experimentally determined value of 1.2 mT was adopted from the literature.[47] This value was obtained for a radical pair with a secondary alkyl radical and a ketyl radical. Due to the similarity in the radical centers $H_{LOC}$ of our system should be close to this value. $\tau_c$ is merely an effective value which depends on the internal viscosity of the micelle and the temperature

$$\tau_c \propto \eta/kT \qquad (10)$$

Because the qualitative shape of the MFE is very much dependent on $\tau_c$, it is possible to estimate $\tau_c$ by simulation of the MFE.[45] Thus we obtain a $\tau_c$ of 0.17 ns as the best value for the system without salt at 293 K. This value corresponds to that calculated with the Stokes−Einstein relation for the molecule with a diameter of 0.36 nm in the medium of 14.0 cP and is a typical value; e.g. a little larger value of 0.44 ns was obtained in a spin-probe study for a little larger spin-labeled chain molecule (16-doxyl-stearic acid) in the same micelle.[48] The relative change in $\tau_c$ for a different condition was estimated from the ESR line shape of the spin adduct obtained with the PBN spin trap using the following equation.[49]

$$\tau_c \propto \Delta H((h_0/h_{-1})^{1/2} + (h_0/h_1)^{1/2} - 2) \qquad (11)$$

where $h_{-1}$, $h_0$, and $h_1$ represent the amplitudes of the three nitrogen hyperfine components of the ESR spectrum of the spin addcut; $\Delta H$ is the line width of the central line. We adopted PBN for this purpose since the spin adduct of the SDS radical obtained with the PBN spin trap resides inside the micelle.[50] The intersystem crossing rate $k_{ISC}$ is postulated as being $A/2\pi$ ($=6.2 \times 10^7$ s$^{-1}$), where $A$(=2.2 mT) represents the average separation between the ESR fields of the two component radicals. This rate is rapid enough and does not give an appreciable change in the simulation even if it was doubled or halved. We estimated the microwave amplitude as being 0.45 mT for the output power of 10 W. Although the microwave power affects little on the PYESR amplitude since the microwave effect saturates at around this power,[33] it gives some effects on the observed kinetics in experiment 1.[16] Since the microwave power employed in this work corresponds to the transition rate of $8.0 \times 10^6$ s$^{-1}$ ($=\gamma B_1/2\pi$), it may be difficult to obtain an accurate $k_H$ much larger than $1.0 \times 10^7$ s$^{-1}$.

## 4. Results and Discussion

The parameters for the reaction scheme (reactions 2, 4, 5, and 7) have been obtained with the pulse-PYESR technique, including the simulation of the time-domain responses. Examples of the pulse-PYESR response for the present system at 289 and 323 K are shown in Figure 1. The time constants of the growth-up process (experiment 1) are about 760 and 260 ns, respectively. From the lower diagram we learn that the lifetime of the RP in the $T_\pm$ states decreases from 2.6 to 1.15 $\mu$s with the increase in the temperature from 289 to 323 K. Through simulation of these curves and those obtained at different temperatures, we obtained the kinetic rate constants listed in Table 1. The escape rate ($k_{ESC}$) and the spin trapping rate ($k_{ST}$) were determined from two independent experiments with different spin trap concentrations (e.g. 1.0 and 3.0 mM). Figure 2 shows $k'_{ST}$, $k_{ESC}$, and $k_{RLX}$ for the above system as functions of temperature. Here $k'_{ST}$ represents the product of $k_{ST}$ and the concentration of DBNBS. These three processes contribute to the decay kinetics observed in experiment 2. It is

**TABLE 1: Kinetic Parameters of the Transient Radical Pair Determined by Simulation of the Pulse-PYESR Response for the Photolysis of Anthraquinone in SDS Micellar Solution at Various Temperatures (NaCl Not Added)[a]**

| | T/K | | | | | | |
|---|---|---|---|---|---|---|---|
| | 289 | 293 | 303 | 313 | 323 | 328 | 333 |
| $\tau_{RP}$[b] | 2.6 | 2.1 | 1.8 | 1.6 | 1.4 | 1.15 | 1.15 |
| $k_P$ | 12 | 16 | 20 | 23 | 29 | 29 | 38 |
| $k_H$ | 2.5 | 6.0 | 7.0 | 8.0 | 11 | 16 | 20 |
| $k_{ESC}$ | 0.1 | 0.15 | 0.19 | 0.26 | 0.38 | 0.43 | 0.43 |
| $k_{ST}$[c] | 0.23 | 0.24 | 0.27 | 0.27 | 0.27 | 0.34 | 0.30 |
| $k_{RLX}$ | 0.077 | 0.077 | 0.082 | 0.087 | 0.093 | 0.1 | 0.11 |
| $\tau_c$[d] | 0.17 | 0.17 | 0.16 | 0.15 | 0.14 | 0.13 | 0.12 |

[a] In units of $10^6$ $s^{-1}$ unless otherwise specified. Concentrations of SDS, anthraquinone, and DBNBS are 100, 0.05, and 1.0 mM, respectively. [b-d] In units of $10^{-6}$ s, $10^9$ $M^{-1}$ $s^{-1}$, and $10^{-9}$ s, respectively.

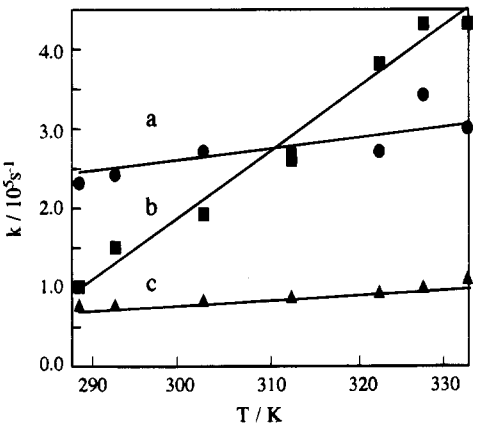


**Figure 2.** Temperature dependence of $k'_{ST}$ (a), $k_{ESC}$ (b), and $k_{RLX}$ (c), which are the rates of dynamic processes contributing to the decay of the RP in the $T_{\pm1}$ states. $k'_{ST}$ represents the pseudo-first-order rate constant of spin trapping (i.e., $k_{ST}$[ST]) at the spin trap concentration of $10^{-3}$ M. Concentrations of SDS, AQ, and DBNBS are 100, 0.06, and 1.0 mM, respectively.

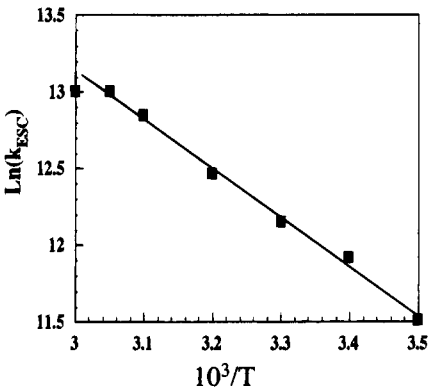


**Figure 3.** Arrhenius plot of $k_{ESC}$ for the system without NaCl addition. Concentrations of SDS, AQ, and DBNBS are 100, 0.06, and 1.0 mM, respectively.

noteworthy that the slope of $k_{ESC}$ is much larger than that of $k'_{ST}$. This fact indicates the two parameters, $k_{ESC}$ and $k'_{ST}$ are dependent on different kinetic processes of the micelle. The fact that the contribution of $k_{RLX}$ is small in the decay kinetics of the radical pair is merely due to a relatively high viscosity inside the micelle which suppresses the motion of the radicals. The Arrhenius plot for $k_{ESC}$ shown in Figure 3 yielded the activation energy of 6.4 kcal/M.

The pulse-PYESR responses were also observed for the system with NaCl added at the concentrations of 0.0, 0.2, and 0.5 M/L. Through simulation of the time-domain signals, in the same manner as described above, the kinetic parameters

**TABLE 2: Kinetic Parameters of the Transient Radical Pair Determined by Simulation of the Pulse-PYESR Response for the Photolysis of Anthraquinone in SDS Micellar Solution at 293 K with Addition of NaCl[a]**

| | $C_{NaCl}$/M | | |
|---|---|---|---|
| | 0.0 | 0.2 | 0.5 |
| $\tau_{RP}$[b] | 2.1 | 1.4 | 0.85 |
| $k_P$ | 16 | 10 | 6.8 |
| $k_H$ | 6.0 | 6.0 | 5.0 |
| $k_{ESC}$ | 0.15 | 0.22 | 0.72 |
| $k_{ST}$[c] | 0.24 | 0.53 | 1.0 |
| $k_{RLX}$ | 0.077 | 0.065 | 0.062 |
| $\tau_c$[d] | 0.17 | 0.20 | 0.21 |

[a] In units of $10^6$ $s^{-1}$ unless otherwise specified. Concentrations of SDS, anthraquinone, and DBNBS are 100, 0.05, and 1.0 mM, respectively. [b-d] In units of $10^{-6}$ s, $10^9$ $M^{-1}$ $s^{-1}$, and $10^{-9}$ s, respectively.

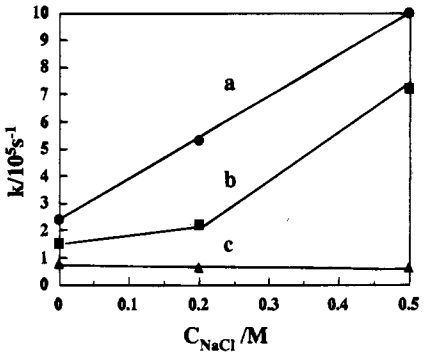


**Figure 4.** NaCl-concentration dependence of the three rates, $k'_{ST}$ (a), $k_{ESC}$ (b), and $k_{RLX}$ (c), which affect the decay rate of the RP in the $T_{\pm1}$ spin states. $k'_{ST}$ represents the pseudo-first-order rate constant of spin trapping at the spin trap concentration of $10^{-3}$ M. The temperature is 293 K. Concentrations of SDS, AQ, and DBNBS are 100, 0.06, and 1.0 mM, respectively.

**TABLE 3: Kinetic Parameters of the Transient Radical Pair Determined by Simulation of the Pulse-PYESR Response for the Photolysis of Anthraquinone in SDS Micellar Solution at Three Temperatures (NaCl Added at 0.2 M)[a]**

| | T/K | | |
|---|---|---|---|
| | 293 | 313 | 333 |
| $\tau_{RP}$[b] | 1.4 | 1.0 | 0.7 |
| $k_P$ | 10 | 16 | 18 |
| $k_H$ | 6.0 | 10 | 20 |
| $k_{ESC}$[e] | 0.22 | 0.35 | 0.52 |
| $k_{ST}$ | 0.53 | 0.68 | 0.85 |
| $k_{RLX}$ | 0.065 | 0.077 | 0.087 |
| $\tau_c$[d] | 0.20 | 0.17 | 0.15 |

[a] In units of $10^6$ $s^{-1}$ unless otherwise specified. Concentrations of SDS, anthraquinone, and DBNBS are 100, 0.05, and 1.0 mM, respectively. [b-d] In units of $10^{-6}$ s, $10^9$ $M^{-1}$ $s^{-1}$, and $10^{-9}$ s, respectively.

listed in Table 2 have been obtained. Figure 4 shows $k'_{ST}$, $k_{ESC}$, and $k_{RLX}$ as the functions of NaCl concentration. An inflection observed for $k_{ESC}$ indicates an additional process occurs for the escape process at the higher NaCl concentrations. Finally, Table 3 lists the kinetic parameters for the system with 0.2 M NaCl at three temperatures of 293, 313, and 333 K. Plots of $k'_{ST}$, $k_{ESC}$, and $k_{RLX}$ are given in Figure 5 as functions of the temperature. The temperature dependence of $k_{ESC}$ becomes smaller while that of $k'_{ST}$ is larger compared with those shown in Figure 2.

**4.1. Molecular Model of Escape Process.** In the following sections we assume that anthrasemiquinone remains in a micelle all the time in our time domain, since it is not very soluble in the aqueous phase, and also that the SDS radical behaves in just the same way as an SDS monomer. In previous work we

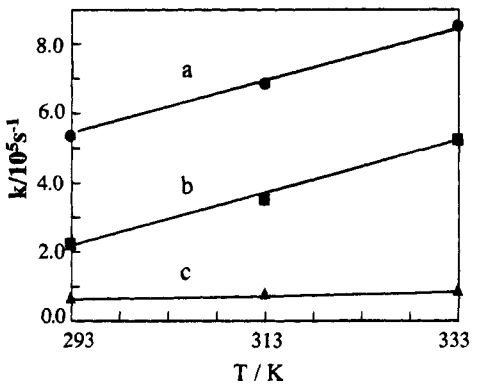


**Figure 5.** Temperature dependence of $k'_{ST}$ (a), $k_{ESC}$ (b), and $k_{RLX}$ (c), which affect the decay rate of the RP in the $T_{\pm 1}$ spin states, for the system with NaCl added at 0.2 M. $k'_{ST}$ represents the pseudo-first-order rate constant of spin trapping at the spin trap concentration of $10^{-3}$ M. Other concentrations are 100, 0.06, and 1.0 mM for SDS, AQ, and DBNBS, respectively.

suggested two mechanisms which contribute the escape process of the RP,[34] i.e. SDS monomer exchange between the micelle and the bulk aqueous phase[12] and fusion/fission of the micelles.[16] The former proceeds as

$$A_n \underset{k_+}{\overset{k_-}{\leftrightarrow}} A_{n-1} + A_1(\mathrm{aq}) \tag{12}$$

$$k_- = c_1 k_+ \tag{13}$$

$$k_- \propto \exp(-\epsilon/kT) \tag{14}$$

where $A_n$ (where the suffix represents the aggregation number) and $A_1$ represent the micelle and monomer, respectively. $c_1$ is the monomer concentration which is close to the cmc (critical micelle concentration) at a low detergent concentration, but decreases considerably with either an increase in the detergent concentration[36] or an addition of salt. $k$ is Boltzmann's factor, $T$ is the temperature, and $\epsilon$ is the activation enthalpy for transferring an SDS molecule out of the micelle. The escape rate for the micelle radical by this mechanism is given as

$$k_{ESC}(\text{monomer exchange}) = k_-/n \tag{15}$$

Using relations (13) and (15), the escape rate is related with the rate of intake of an SDS monomer by the micelle ($k_+$):

$$k_+ \sim k_{ESC}(n/c_1) \tag{16}$$

The other process which contributes to the escape rate is the fusion/fission process of the micelle:[34]

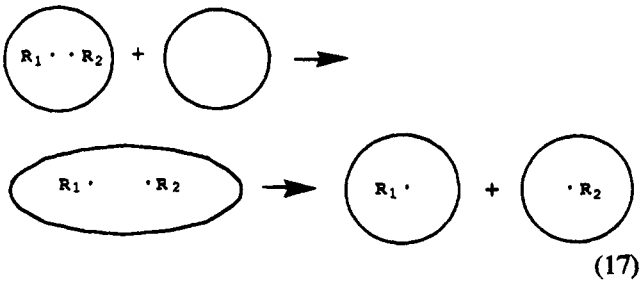


(17)

Here, the micelle including a RP fuses into a larger micelle upon collision with another micelle. In a short time, fission of this large micelle occurs due to instability and the two radicals are separated at the probability of $^1/_2$.

**4.2. Temperature Dependence.** According to Figure 2, $k_{ESC}$ increases significantly with increasing temperature from 289 to 333 K. On the other hand the temperature dependence of $k_{ST}$, the rate of spin trapping, is very small. This fact indicates that the rate of spin trapping directly from the RP depends on micellar dynamics other than the above processes. If the radical center is temporarily out of or near to the surface of the micelle upon collision of a spin trap, the SDS radical may be trapped. A smaller activation energy for $k_{ST}$ compared with that of $k_{ESC}$ is reasonable, since the energy to pull an SDS monomer completely out of the micelle to achieve the escape process should be much larger than that for changing the disposition of the SDS radical in the micelle to make contact with the spin trap.

The rate of recombination reaction ($k_P$) also increases with the temperature, from $1.2 \times 10^7$ s$^{-1}$ at 289 K to $3.8 \times 10^7$ s$^{-1}$ at 333 K (Table 1). This may be due to the thermal activation of both the lateral diffusion in the micelle and the rotational diffusion of the two radicals. The latter is necessary for the pair of radicals to achieve an appropriate conformation for recombination. This parameter $k_P$ is obtained to fit the maximum PYESR effect with the calculated value, which is mainly determined by the ratio of $k_P$ and $k_{ESC}$: an increase in $k_P/k_{ESC}$ causes an increase in the calculated PYESR amplitude. A large increase in $k_H$ was observed with an increase in the temperature. If the excited triplet state is quenched exclusively by the hydrogen abstraction reaction, $k_H$ obtained in our method represents the hydrogen abstraction rate. However, since fitting of the growth process, which usually finishes in less than 1.0 $\mu$s, is rather difficult and there might exist other processes for the quenching of the excited triplet anthraquinone, we cannot give a high credit for the absolute values of this parameter.

**4.3. EFfect of NaCl.** Addition of NaCl causes changes in size and shape of the micelle. At a low concentrations of NaCl below 0.2 M the micelle keeps the spherical shape and its radius does not increase very much.[37,38] With increasing NaCl concentration to say 0.5 M, the effective radius increases very much especially at low temperatures. This increase accompanies the shape change from sphere to rod. The viscosity inside the micelle may also change. These physico-chemical changes of the micelle as well as the change in the dynamics of the SDS monomer should affect our observations. Inputting the observed $k_{ESC}$ of about $2.0 \times 10^5$ s$^{-1}$ for the system with 0.2 M NaCl at 293 K, together with less than $1.0 \times 10^{-3}$ M for $c_1$, and $n \sim 100$ into eq 16, we obtain $k_+ \sim 2.0 \times 10^{10}$ M$^{-1}$ s$^{-1}$. Since this value is a few times larger than the diffusion limit value, it is impossible to explain this only with the monomer exchange process. We have proposed the fusion/fission process for another mechanism of $k_{ESC}$ to avoid this difficulty, although at a low SDS concentration and without any additives the cross section of fusion is suppressed to be small due to the electrostatic repulsion.[34] At a high $Na^+$ concentration the electrostatic repulsion between micelles decreases and the fusion/fission process may become important for the micelle dynamics. A similar model has been proposed to explain the relaxation process in the micellar solution.[51] In addition, in place of the fusion/fission mechanism, the monomer exchange process maybe stimulated by a strong collision in which several or more monomers are exchanged between the two micelles upon one occasion.[52] However, we may not be able to discriminate between the two mechanisms, i.e. the fusion/fission and the strong collision mechanisms.

Since a distinct inflection is found in the NaCl-concentration dependence of $k_{ESC}$ between 0.2 and 0.5 M, we have to consider one more mechanism. At 0.5 M NaCl the effective diameter

of the micelle becomes as large as 8.0 nm at 298 K,[37,38] which indicates that the shape is no longer spherical but rodlike. In this situation we have to consider the possibility that, even if the two radicals remain in the micelle, the RP is regarded as being separated into component radicals, if there is little chance to meet again within our time domain. This means an escape process within the micelle. This is necessary since even if collision between micelles occurs at the diffusion limit rate, the calculated rate for the fusion/fission process cannot explain the large $k_{ESC}$ of $7.2 \times 10^5$ $s^{-1}$ at the NaCl concentration of 0.5 M. If $n$ becomes larger than 600 ($r = 8$ nm; micelle concentration $< 2 \times 10^{-4}$ M),[37,38] $k_{ESC}$ exceeds the diffusion limit value for the rate of the fusion/fission process. However, we need another volume of experimental data to discuss this mechanism more.

The effect of salt on the spin trapping rate $k_{ST}$ is still larger (Figures 4 and 5) compared with that on $k_{ESC}$, even with addition of 0.2 M NaCl. In contrast to the small temperature dependence for the system without NaCl, that for the system with 0.2 M NaCl becomes much larger (Figure 5). In addition, $k_{ST}$ at 333 K for the system without NaCl ($3.0 \times 10^8$ $M^{-1}$ $s^{-1}$) is much smaller than $k_{ST}$ at 293 K with the addition of 0.2 M NaCl ($5.3 \times 10^8$ $M^{-1}$ $s^{-1}$). This fact means that an additional mechanism, to which a higher activation energy is assigned, becomes important. For example temporal incorporation of the spin trap into the micelle is a candidate for this mechanism. This becomes possible when the electrostatic repulsion between the negative charges of the spin trap and the SDS micelle is reduced by NaCl. In this case the activation energy may be that which is necessary for the spin trap to break into the micelle through the Stern layer.

A decrease in $k_P$ is noticeable upon addition of NaCl. One reason is the increase in the volume of the micelle, which reduces the chance for the component radicals to meet again to react. Another possibility is the increase in viscosity of the interior of the micelle. Although the correlation time determined from the ESR line width increases a little (Tables 1−3) upon addition of NaCl, this change in viscosity is far smaller than that which explains the observed $k_P$. Thus, the largest contribution may come from the former.

**Acknowledgment.** This work was partly supported by Special Coordination Funds for Promoting Science and Technology. This work was also supported by a Grant-in-aid for Scientific Research on Priority Area "Molecular Magnetism" (Area No. 228/04242102) from the Ministry of Education, Science, and Culture of Japan.

## References and Notes

(1) Salikhov, K. M.; Molin, Yu. N.; Sagdeev, R. Z.; Buchanchenko, A. L. *Spin Polarization and Magnetic Effect in Radical Reactions;* Elsevier: Amsterdam, 1984.
(2) Hayashi, H. In *Photochemistry and Photophysics;* Rabek, J. F., Ed.; CRC Press: Boca Raton, FL, 1990; Vol. 1, pp 59−136.
(3) Steiner, U. E.; Wolff, H.-J. In *Photochemistry and Photophysics;* Rabek, J. F., Ed.; CRC Press: Boca Raton, FL, 1991; Vol. 4, pp 1−130.
(4) Turro, N. J. *Proc. Natl. Acad. Sci. U.S.A.* **1983**, *80*, 609.
(5) Sakaguchi, Y.; Nagakura, S.; Hayashi, H. *Chem. Phys. Lett.* **1980**, *72*, 420.
(6) Tanimoto, Y.; Udagawa, H.; Itoh, M. *J. Phys. Chem.* **1983**, *87*, 724.
(7) Turro, N. J.; Cherry, W. R. *J. Am. Chem. Soc.* **1978**, *100*, 7431.
(8) Tanimoto, Y.; Takashima, M.; Itoh, M. *J. Phys. Chem.* **1984**, *88*, 6053.
(9) Kaptein, R.; Oosterhoff, L. J. *Chem. Phys. Lett.* **1969**, *4*, 214.
(10) Closs, G. L.; Trifunac, A. D. *J. Am. Chem. Soc.* **1970**, *92*, 2184.
(11) Okazaki, M.; Shiga, T. *Nature* **1986**, *323*, 240.
(12) Closs, G. L.; Forbes, M. D. E.; Norris, J. R., Jr. *J. Phys. Chem.* **1987**, *91*, 3592.
(13) Buckley, C. D.; Hunter, D. A.; Hore, P. J.; McLauchlan, K. A. *Chem. Phys. Lett.* **1987**, *135*, 307.
(14) Sakaguchi, Y.; Hayashi, H.; Murai, H.; I'haya, Y. J. *Chem. Phys. Lett.* **1984**, *110*, 275.
(15) Okazaki, M.; Sakata, S.; Konaka, R.; Shiga, T. *J. Chem. Phys.* **1987**, *86*, 6792.
(16) Okazaki, M.; Toriyama, K. *Bull. Chem. Soc. Jpn.* **1993**, *66*, 1892.
(17) Turro, N. J.; Buchachenko, A. L.; Tarasov, V. F. *Acc. Chem. Res.* **1995**, *28*, 69.
(18) Janzen, E. G. *Acc. Chem. Res.* **1971**, *4*, 31.
(19) Lagercrantz, C. *J. Phys. Chem.* **1971**, *75*, 3466.
(20) Okazaki, M.; Konishi, Y.; Toriyama, K. *Chem. Lett.* **1994**, 737.
(21) Lersch, W.; Michel-Beyerle, M. E. In *Advanced EPR;* Hoff, A. J., Ed.; Elsevier: Amsterdam, 1989; Chapter 19.
(22) Lepine, D. *Phys. Rev. B* **1972**, *6*, 436.
(23) Frankevich, E. L.; Pristupa, A. I.; Lesin, V. I. *Chem. Phys. Lett.* **1977**, *47*, 304.
(24) Cavenett, B. C. *Adv. Phys.* **1980**, *30*, 475.
(25) Molin, Yu. N.; Anisimov, O. A.; Grigoryants, V. M.; Molchanov, V. K.; Salikhov, K. M. *J. Phys. Chem.* **1980**, *84*, 1853.
(26) Smith, J. P.; Trifunac, A. D. *J. Phys. Chem.* **1981**, *85*, 1645.
(27) Bowman, M. K.; Budil, D. E.; Closs, G. L.; Kostka, A. G.; Wraight, C. A.; Norris, J. R. *Proc. Natl. Acad. Sci., U.S.A.* **1981**, *78*, 3305.
(28) Batchelor, S. N.; Shkrob, I. A.; McLauchlan, K. A. *J. Phys. Chem.* **1991**, *95*, 4940.
(29) Okazaki, M.; Tai, Y.; Nakagaki, R.; Nunome, K.; Toriyama, K. *Chem. Phys. Lett.* **1990**, *166*, 227.
(30) Bagryanskaya, E. G.; Grishin, Yu. A.; Sagdeev, R. Z. *Chem. Phys. Lett.* **1985**, *113*, 234.
(31) Polyakov, N. E.; Konishi, Y.; Okazaki, M.; Toriyama, K. *J. Phys. Chem.* **1994**, *98*, 10558.
(32) Okazaki, M.; Polyakov, N. E.; Konishi, Y.; Toriyama, K. *Appl. Magn. Reson.* **1994**, *7*, 149.
(33) Okazaki, M.; Toriyama, K. *J. Phys. Chem.* **1995**, *99*, 489.
(34) Okazaki, M.; Polyakov, N. E.; Toriyama, K. *J. Phys. Chem.* **1995**, *99*, 6452.
(35) Konishi, Y.; Okazaki, M.; Toriyama, K. *J. Phys. Chem.* **1995**, *99*, 12540.
(36) Kahlweit, M.; Teubner, M. *Adv. Colloid Interface Sci.* **1981**, *13*, 1.
(37) Mazer, N. A.; Benedek, G. B.; Carey, M. C. *J. Phys. Chem.* **1976**, *80*, 1075.
(38) Missel, P. J.; Mazer, N. A.; Benedek, G. B.; Carey, M. C. *J. Phys. Chem.* **1983**, *87*, 1264.
(39) Turro, N. J.; Okubo, T. *J. Am. Chem. Soc.* **1981**, *103*, 7224.
(40) Kaur, H.; Leung, K. W. H.; Perkins, M. J. *J. Chem. Soc., Chem. Commun.* **1981**, 142.
(41) Okazaki, M.; Sakata, S.; Konaka, R.; Shiga, T. *J. Am. Chem. Soc.* **1985**, *107*, 7214.
(42) Okazaki, M.; Sakata, S.; Konaka, R.; Shiga, T. *J. Phys. Chem.* **1987**, *91*, 1131.
(43) Brocklehurst, B. *J. Chem. Soc., Faraday Trans. 2* **1976**, *72*, 1869.
(44) Hayashi, H.; Nagakura, S. *Bull. Chem. Soc. Jpn.* **1984**, *57*, 322.
(45) Okazaki, M.; Tai, Y.; Nunome, K.; Toriyama, K.; Nagakura, S. *Chem. Phys.* **1992**, *161*, 177.
(46) Carrington, A.; McLachlan, A. D. In *Introduction to Magnetic Resonance;* Harper & Row: New York, 1967; Chapter 11.
(47) Tanimoto, Y.; Fujiwara, Y. ;Takamatsu, S.; Itoh, M.; Okazaki, M. *J. Phys. Chem.* **1992**, *96*, 9844.
(48) Baglioni, P.; Rivara-Minten, E.; Dei, L.; Ferroni, E. *J. Phys. Chem.* **1990**, *94*, 8218.
(49) Nordio, P. L. In *Spin Labelling Theory and Applications;* Berliner, L. J., Ed.; Academic Press: New York, 1976; Chapter 2.
(50) Janzen, E. G.; Coulter, G. A. *J. Am. Chem. Soc.* **1984**, *106*, 1962.
(51) Lessner, E.; Teubner, M.; Kahlweit, M. *J. Phys. Chem.* **1981**, *85*, 3167.
(52) Tachiya, M. *Kinetics of Nonhomogeneous Processes;* Freeman, G. R., Ed.; John-Wiley: New York, 1987; Chapter 11.

JP951444Y